Development/Plasticity/Repair

Transporter Protein-Coupled DPCPX Nanoconjugates Induce Diaphragmatic Recovery after SCI by Blocking Adenosine A1 Receptors

Zeljka Minic,[1]* Yanhua Zhang,[2]* Guangzhao Mao,[2] and Harry G. Goshgarian[1]

[1]Wayne State University School of Medicine, Department of Anatomy and Cell Biology, Detroit, Michigan 48201, and [2]Wayne State University College of Engineering, Department of Chemical Engineering and Materials Science, Detroit, Michigan 48202

Respiratory complications in patients with spinal cord injury (SCI) are common and have a negative impact on the quality of patients' lives. Systemic administration of drugs that improve respiratory function often cause deleterious side effects. The present study examines the applicability of a novel nanotechnology-based drug delivery system, which induces recovery of diaphragm function after SCI in the adult rat model. We developed a protein-coupled nanoconjugate to selectively deliver by transsynaptic transport small therapeutic amounts of an A1 adenosine receptor antagonist to the respiratory centers. A single administration of the nanoconjugate restored 75% of the respiratory drive at 0.1% of the systemic therapeutic drug dose. The reduction of the systemic dose may obviate the side effects. The recovery lasted for 4 weeks (the longest period studied). These findings have translational implications for patients with respiratory dysfunction after SCI.

Key words: **motor systems; nanotechnology; phrenic nucleus; plasticity; respiratory recovery; spinal cord injury**

Significance Statement

The leading causes of death in humans following SCI are respiratory complications secondary to paralysis of respiratory muscles. Systemic administration of methylxantines improves respiratory function but also leads to the development of deleterious side effects due to actions of the drug on nonrespiratory sites. The importance of the present study lies in the novel drug delivery approach that uses nanotechnology to selectively deliver recovery-inducing drugs to the respiratory centers exclusively. This strategy allows for a reduction in the therapeutic drug dose, which may reduce harmful side effects and markedly improve the quality of life for SCI patients.

Introduction

Spinal cord hemisection caudal to the C2 dorsal roots (C2Hx) interrupts the descending bulbospinal respiratory pathways, thereby causing life-threatening weakness of the respiratory muscles. Indeed, respiratory problems, such as pneumonia, septicemia, and pulmonary emboli, are leading causes of death in humans after SCI (Winslow and Rozovsky, 2003). It is important to understand the mechanisms/pathways related to recovery of respiratory function after the injury.

Inspiratory drive to phrenic motoneurons originates within the rostral ventral respiratory group (rVRG) of neurons in the medulla (Fig. 1). In rats, these bulbospinal neurons send their axons to the phrenic nuclei located at the C3-C6 segments to depolarize the phrenic motoneurons (DeVries and Goshgarian, 1989). We have shown that the descending bulbospinal pathways have spinal decussating collaterals, which project to both phrenic nuclei in the rat (Moreno et al., 1992). These collaterals are known as the crossed phrenic pathway (CPP), and this pathway is normally latent. A C2Hx interrupts the major bulbospinal pathways and results in paralysis of the ipsilateral hemidiaphragm (Aserinsky, 1961; Guth, 1976). Function of the paralyzed hemidiaphragm can be restored by activating the latent CPP. A single intravenous administration of the

Received June 30, 2015; revised Jan. 6, 2016; accepted Jan. 8, 2016.

Author contributions: G.M. and H.G.G. designed research; Z.M. and Y.Z. performed research; Y.Z. and G.M. contributed unpublished reagents/analytic tools; Z.M. analyzed data; Z.M., G.M., and H.G.G. wrote the paper.

This work was supported by National Institute of Health Grant HD-31550 to H.G.G. The work presented herein has been submitted for patenting: "Transporter Protein-Coupled Nanodevices for Targeted Drug Delivery," First Named Inventor/Applicant Name: Harry Goshgarian (coinventors: Guangzhao Mao, Yanhua Zhang). Application number: 14/534,994, Application type: Utility/Design using an application data sheet (37 CFR 1.76), Date Filed: November 6, 2014. Wayne State University owns the patent. We thank Dr. Thomas Sanderson from the Department of Emergency Medicine at Wayne State University and his laboratory for making the microscopy equipment available for our use and for his technical expertise in acquiring images.

The authors declare no competing financial interests.

*Z.M. and Y.Z. contributed equally to this study.

Correspondence should be addressed to Dr. Harry G. Goshgarian, Department of Anatomy and Cell Biology, Wayne State University, School of Medicine, 540 East Canfield Avenue, Detroit, MI 48201. E-mail: hgoshgar@med.wayne.edu.

DOI:10.1523/JNEUROSCI.2577-15.2016

Copyright © 2016 the authors 0270-6474/16/363441-12$15.00/0

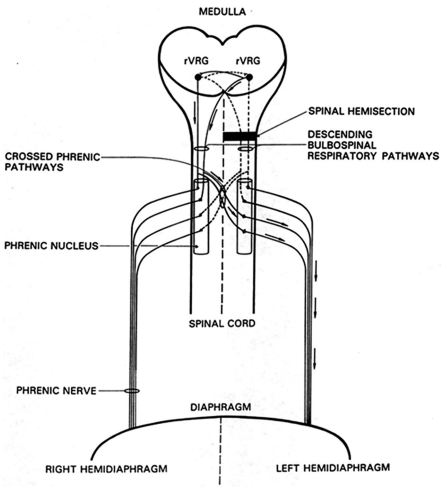

Figure 1. The respiratory motor pathways involved in the "crossed phrenic phenomenon." Respiratory drive originates in the rVRG in the medulla, and these neurons descend bilaterally to the phrenic motor nuclei. Both ipsilateral and contralateral descending pathways have collaterals that project to both phrenic nuclei. These collaterals are also known as the CPP. Hemisection rostral to the phrenic motor nucleus interrupts (dotted lines) the nerve traffic from the descending bulbospinal respiratory pathways and effectively paralyzes the hemidiaphragm ipsilateral to the hemisection. Arrows indicate pathways that neural impulses follow to restore respiratory function after the hemisection. These pathways are initially latent under normal conditions but can be activated via drugs that increase central respiratory drive, such as DPCPX or theophylline. Reprinted from Nantwi and Goshgarian (2005) with permission from Neurological Research.

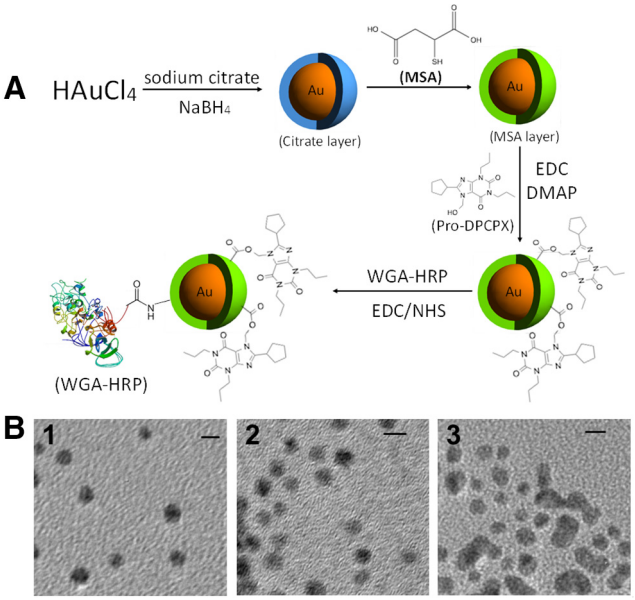

Figure 2. ***a***, Step-by-step synthesis of the tripartite nanoconjugate comprised of a 4 nm AuNP carrier coupled to a transporter protein (WGA-HRP) and to the drug (DPCPX). ***b***, Transmission electron microscopy images of step-by-step protein-AuNP-drug nanodevice formation: (1) AuNP only, (2) AuNP-DPCPX, and (3) WGA-HRP-AuNP-DPCPX. Calibration: 5 nm.

adenosine receptor antagonist, theophylline, activated the CPP and induced recovery of the paralyzed hemidiaphragm in rats (Nantwi et al., 1996). Additionally, multiple oral administrations of theophylline induced plasticity in the respiratory centers, which resulted in permanent recovery of the paralyzed hemidiaphragm in rats, lasting weeks after the animals were weaned from the drug (Nantwi et al., 2003). Studies of this systemic therapeutic intervention in patients with SCI yielded positive effects on respiratory function (Ferguson et al., 1999; Bascom et al., 2005); however, theophylline also caused undesirable side effects (i.e., vomiting, nausea, and insomnia), which ultimately resulted in many of the patients dropping out of a double-blinded, placebo-controlled crossover trial (Tzelepis et al., 2006). The deleterious effects were caused by the action of the drug on several other CNS centers and not the drug's action on the respiratory nuclei (Barnes, 2013).

The objective of the present study was to develop a technique that delivers recovery-inducing drugs to the respiratory centers only, bypassing all other nonrespiratory sites. In developing the technique of selective drug delivery, we found that we could significantly reduce the dosage of the drug necessary to induce recovery of the diaphragm compared with systemic administration. This obviates the need for systemic drug administration, which causes side effects. Specifically, we developed a tripartite nanoconjugate comprised of a gold nanoparticle (AuNP) coupled to a transporter protein (WGA-HRP) and to the drug, 1,3-dipropyl-8-cyclopentylxantine (DPCPX), which is a selective antagonist of A1 adenosine receptors (Lohse et al., 1987). Like theophylline, DPCPX, when injected systemically, can induce recovery of the paralyzed hemidiaphragm in C2Hx rats (Nantwi and Goshgarian, 2002). We chose the AuNP as the drug carrier because its conjugation chemistry with drugs and proteins as well as its biomedical applications have been well documented (Dreaden et al., 2011; Mieszawska et al., 2013). Despite ongoing preclinical and clinical trials of various nanotherapies, the ability to target drugs to areas affected by disease *in vivo* remains to be limited (Etheridge et al., 2013). In the current study, the nanoconjugate is injected into the paralyzed hemidiaphragm of C2Hx rats. The transporter component of the nanoconjugate (WGA-HRP) is taken up by phrenic axon terminals through receptor-mediated endocytosis and transported retrogradely to the phrenic nucleus. Subsequently, the nanoconjugate is carried by WGA-HRP transsynaptically to the cells in the rVRG over functionally active synapses (Moreno et al., 1992). WGA-HRP does not transport to any other CNS center in the acutely injured animal. In the present study, the nanoconjugate was purposefully designed with bonds that would allow DPCPX to become disassociated from the AuNP carrier once the nanoconjugate reached the respiratory centers. The DPCPX drug then becomes active. The action of the drug itself on inducing respiratory-related recovery and diaphragm contractility has been described previously (Kajana and Goshgarian, 2008a).

Materials and Methods

Nanoconjugate synthesis

Chemicals used in the synthesis of the DPCPX nanoconjugate were purchased from Sigma-Aldrich: gold(III) chloride trihydrate ($HAuCl_4 \cdot 3H_2O$, 99% metal trace), sodium citrate tribasic dehydrate (98%), mercaptosuccinic acid (MSA, 97%), sodium borohydride ($NaBH_4$, 98%), 4-dimethylaminopyridine (99%), DMSO (99.8%), 37% formaldehyde solution, tetrahydrofuran (99%), N-hydroxysuccinimide (98%), and DPCPX (97%), lectin from triticum vulgaris (WGA-HRP). Finally,1-ethyl-3-(3-dimethylaminopropyl) carbodiimide (98%) was purchased from Fluka Analytical. The synthesis steps of the nanoconjugate are described in Figure 2*a*. MSA-capped AuNP was prepared according to the literature (Jana et al., 2001). The proform of DPCPX (pro-DPCPX) was synthesized based on the Mannich reaction (Sloan and Bodor, 1982). The pro-DPCPX was loaded on to the MSA-capped AuNP through an esterification reaction to yield the AuNP-DPCPX nanoconjugate. Then WGA-HRP was chemically bonded to AuNP-DPCPX through an amide bond.

Animal studies

All protocols and surgical procedures used in this study were reviewed and approved by the Wayne State University Institutional Animal Care

and Use Committee and were performed in accordance with the *Guide for the Care and Use of Laboratory Animals* published by the National Institutes of Health.

Experimental design

Ten-week old male, Sprague Dawley rats ($n = 59$) were randomized into treated and control groups. On day 0, all rats were subjected to left C2Hx. Immediately following the C2Hx on day 0, rats in the treated groups were injected into the left hemidiaphragm (LHD) with the tripartite nanoconjugate composed of WGA-HRP, AuNP, and DPCPX in a dose-dependent manner: 0.09 μg/kg ($n = 10$), 0.15 μg/kg ($n = 15$), or 0.27 μg/kg ($n = 10$). Rats within the control groups were injected with control solutions containing either WGA-HRP-AuNP (no drug) ($n = 10$) or AuNP-DPCPX (no WGA-HRP) ($n = 4$). All the injection volumes were adjusted based on animal weight. A subset of animals ($n = 3$) underwent C2Hx and received no intradiaphragmatic injections to test for the presence of spontaneous recovery in the current study design, and another subset of animals ($n = 4$) received no C2Hx and were injected with DPCPX nanoconjugate (0.15 μg/kg). In addition, three rats were prepared for immunochemistry after injection of the tripartite nanoconjugate as described below.

Perioperative care

Animals were anesthetized with intraperitoneal injections of a ketamine/xylazine mixture (70 mg/kg and 10 mg/kg i.p., respectively). Once anesthetized, the animals were injected intramuscularly with the antiparasympathetic agent, atropine sulfate (0.04 mg/kg), to prevent mucus secretion. Animals were then prepared for aseptic survival surgery according to the Handbook for Laboratory Animal Care and Use.

Left C2 hemisection

On day 0, animals underwent left C2Hx as previously described in our laboratory (Nantwi et al., 1996; Kajana and Goshgarian, 2008a). Briefly, a dorsal incision was made exposing the C2 vertebra. Following laminectomy and durotomy, the left half of the spinal cord was cut just caudal to the C2 roots and extended from the midline to the most lateral aspects of the left side of the spinal cord. The muscles were closed using 3.0 absorbable Vicryl sutures (E-sutures), and skin was stapled using wound clips (Roboz Surgical Instruments).

Electromyography

To verify completeness of the hemisection, electromyography was performed similarly to how it was done previously in our laboratory (Moreno et al., 1992; Nantwi et al., 1996). A 7-cm-long horizontal incision was made 3 cm caudal to the sternum, and bipolar platinum electrodes (Grass E-2B) were inserted into the LHD and right hemidiaphragm (RHD). Raw signals were amplified 20,000 times using a Grass P511 amplifier (Grass Technologies) and filtered at 30 Hz to 3 kHz. Data were acquired using the Spike 2 program (Cambridge Electronic Design system). The muscle and skin were closed using a 3.0 absorbable Vicryl (E-sutures) and wound clips (Roboz Surgical Instruments), respectively. The left hemisection was deemed complete if there was no respiratory-related activity detected in the LHD.

Starting on day 4 and continuing every 4–6 d until day 30, animals were anesthetized and EMG recordings of the LHD were conducted ($n = 56$) to test for the presence of activity in any of the areas of the LHD (anterior, lateral, and posterior). Recordings were also taken from the RHD. No animal was tested >4 times for recovery due to the stress of multiple surgeries.

The nanoconjugate administration

Immediately after verification of completeness of the hemisection through complete paralysis of the LHD, animals received injections based on their weight of either the DPCPX nanoconjugate or control solutions. The injections were equally spread over the posterior, lateral, and anterior areas of the diaphragm using a Hamilton syringe (26S) based on the weight of the animal. A single injection did not exceed 10 μl volume. The quality of each diaphragmatic injection was verified visually; the needle was inserted parallel to the muscle fibers such that the tip of the needle was visualized by eye before administration of the injections. A small bubble was created in the diaphragm where the solution was deposited. The needle was held in place for ~5–10 s before it was withdrawn from the muscle to prevent leakage of the nanoconjugate outside of the diaphragm. Steps were taken to avoid leakage of the solution from the muscle. After administration of the injections, animals were cleaned and prepared for suturing. Muscle was closed using 3.0 absorbable Vicryl threads while the skin was closed using wound clips.

Immunohistochemical visualization of DPCPX nanoconjugate

Following injection of the tripartite nanoconjugate into the hemidiaphragm ipsilateral to C2Hx, the animals were allowed to survive for 48 h ($n = 3$). Following anesthesia as described above, the rats underwent transcardial perfusion using heparinized saline followed by 4% formaldehyde (Fisher, F-79). Spinal segments C3-C6 as well as the medulla were collected and allowed to postfix for 24 h. The tissue was then cryoprotected in 30% sucrose and cut transversely on the cryostat at 50 μm thickness.

The sections containing the phrenic nucleus and the rVRG were washed three times in the immuno buffer (PBS + 0.3% Triton) and then blocked using 10% normal horse serum (Invitrogen) in the immuno buffer. Sections were incubated in primary antibody goat anti-WGA (1:200, AS-2024, Vector Laboratories), diluted in 10% normal horse serum-immuno buffer solution for 72 h, and then washed in PBS (Strack and Loewy, 1990). Washes were followed by incubation in the biotinylated secondary antibody, donkey anti-goat (1:400, Jackson ImmunoResearch Laboratories), overnight. Finally, sections were incubated in streptavidin-tagged-Cy3 for 4 h and then mounted wet on the slides and coversliped.

The images were acquired using a Leica microscope, Zeiss AxioObserver Z1, and the camera, AxioVision MRm. Low-power images were taken using the 2.5× objective. Off-line processing was used to acquire high-power views of the phrenic nuclei and the rVRGs.

Postoperative care

Animals were given buprenorphine hydrochloride (0.02 mg/kg, s.c.) to minimize pain and sterile saline (10 ml, s.c.) to avoid dehydration. Also, Carprofen tablets (2 mg/tablet) were given by mouth to reduce inflammation. The lower abdomen was gently compressed while animals were still anesthetized to induce micturition and defecation. Bowel and bladder functions returned to normal 24 h after the surgery. Animals were left to recover on a heating blanket overnight. Food and water were provided *ad libitum*, and animals were also given cereal and apple slices as an enticement to eat.

Phrenic nerve recordings (nonsurvival surgery)

One week ($n = 8$), two weeks ($n = 8$), or 4 weeks ($n = 10$) following the administration of the nanoconjugate, animals underwent bilateral phrenic nerve recordings under standardized conditions. The procedure used in our laboratory has been described previously (Nantwi and Goshgarian, 2002; Kajana and Goshgarian, 2009). Phrenic nerves were accessed from the ventral surface of the neck and cut distally to eliminate afferent activity. Each nerve was positioned on stainless steel bipolar electrodes and covered in gel (Bisico) to prevent fluid interference with the signal and minimize electrical noise. Before acquiring nerve activity data, the following standardizing conditions were performed: (1) animals were bilaterally vagotomized; (2) animals were paralyzed using pancuronium bromide (0.5 mg/kg); and (3) animals were placed on a ventilator set at 3–5 mmHg above the apnea threshold. The procedure for determining the apnea threshold has been described previously (Kajana and Goshgarian, 2008a, b, 2009). The unprocessed recording was amplified 5000 times using Grass P511 amplifiers (Grass Technologies), filtered at 0.3–1 kHz. The recordings were digitized, rectified, and integrated in 0.1 s intervals using the Cambridge Electronic Design data acquisition system and the Spike 2 software.

Data analysis

Characterization of hemidiaphragm recovery observed with the EMG. We used EMG analysis to determine the proportion of animals in each experimental and control group that experienced recovery in the LHD. We need to stress that we were not attempting to quantitate the amount of

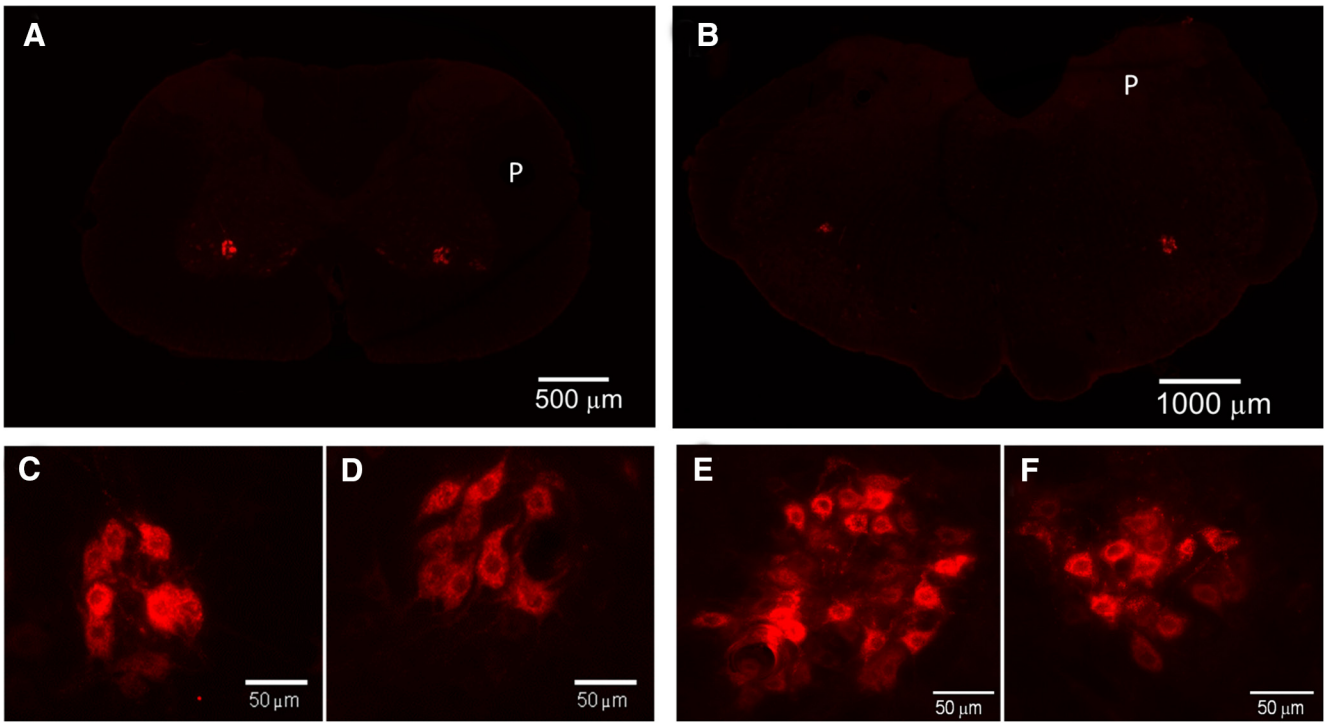

Figure 3. Retrograde transsynaptic transport of the DPCPX nanoconjugate to the phrenic nucleus and to the rVRG. ***a***, Bilateral staining of the phrenic nucleus acquired under low magnification. ***c***, ***d***, High-power images of the specific cells of the phrenic nucleus. ***b***, Bilateral staining of the rVRG. ***e***, ***f***, High-power images of these same cells of the left and right rVRG, respectively. The pinhole (P) is made on the right side of the tissue.

recovery by EMG analysis, but only the incidence of recovery in nanoconjugate-treated animals with respect to the incidence of recovery in the control group. Furthermore, our definition of recovery was specific. Recovery of the LHD was considered positive in each animal only if the following conditions were met: (1) the EMG activity was detected in at least two of the three diaphragm areas (posterior, lateral, and anterior); and (2) if the activity persisted for the duration of the study. In each treatment group, animals were then divided into those having recovery or not, and the Fisher exact test was performed to determine whether the proportion of animals with functional diaphragm recovery in the treated groups was statistically different from the ratio of control animals having recovery. The Fisher's exact test was followed by the Bonferonni adjustment to correct for the number of comparisons tested. The α level of 0.016 was considered statistically significant.

Phrenic nerve recordings. Phrenic nerve recordings were used to estimate the increase in phrenic nerve output after nanoconjugate injections. The recordings were also used to analyze the effect of injection of DPCPX nanoconjugate on respiratory frequency. The areas under 10 consecutive integrated waveforms in the right phrenic nerve (RPN) and left phrenic nerve (LPN) activity were averaged and expressed as mean ± SE. Activity in the left nerve was used as an index of the recovered respiratory activity in the DPCPX nanoconjugate-treated animals. Both maximum LPN amplitude activities as well as the areas under the curves (AUC) were expressed as the percentage of the RPN whose signal was set to be 100%. The data were analyzed using a two-way ANOVA on ranks for independent measures. When appropriate, ANOVA was followed by the Student's independent *t* test. The α level of 0.01 was considered statistically significant. Frequency data are expressed as mean ± SE and were analyzed using two-way ANOVA for independent measures followed by the Student's independent *t* test. The α level of 0.01 was considered statistically significant for this analysis.

Results

Synthesis and characterization of the nanoconjugate

Figure 2*a* shows step-by-step synthesis of the nanoconjugate. The first step in engineering the nanoconjugate was to create AuNPs by reacting gold (III) chloride trihydrate with sodium citrate and sodium borohydrate. In the next step, AuNPs were reacted with MSA (capped nanoconjugate) to allow formation of the functional groups, which would bind the drug (DPCPX) and the transporter (WGA-HRP) in later steps of the fabrication process. Next, the drug was conjugated to the MSA-capped AuNPs through an esterification process. In the final step, the WGA-HRP transporter was bound to the particle using the amide bond. Figure 2*b* shows transmission electron microscopy images of the AuNPs only (1), after they are conjugated with pro-DPCPX (2) and finally with WGA-HRP (3). The average AuNP core size is 4 nm. The amount of the drug conjugated to each AuNP was determined by thermal gravimetric analysis and used to estimate drug dosage.

Retrograde transsynaptic transport of WGA-HRP-AuNP-DPCPX nanoconjugate

Figure 3 provides anatomical proof that, when the nanoconjugate is injected into the diaphragm, it is retrogradely transported to the phrenic nucleus and subsequently transsynaptically transported to the rVRG in the medulla. The WGA-HRP component of the nanoconjugate was visualized 48 h after injection by WGA-HRP immunochemistry (Strack and Loewy, 1990). At this time, there was no recovery detected in these animals. The earliest time recovery detected in other animals was 72 h after nanoconjugate injection. Figure 3*a* is a low-power view showing bilateral staining of WGA-HRP-labeled phrenic motor neurons in the spinal cord, whereas Figure 3*c*, *d* shows a higher magnification of these same labeled cells in the left and right phrenic nuclei, respectively. The bilateral staining is due to diffusion of the WGA tracer across the midline of the diaphragm, as we have demonstrated in a previous study (Buttry and Goshgarian, 2014). The staining is localized to the phrenic nuclei only, suggesting that the nanocon-

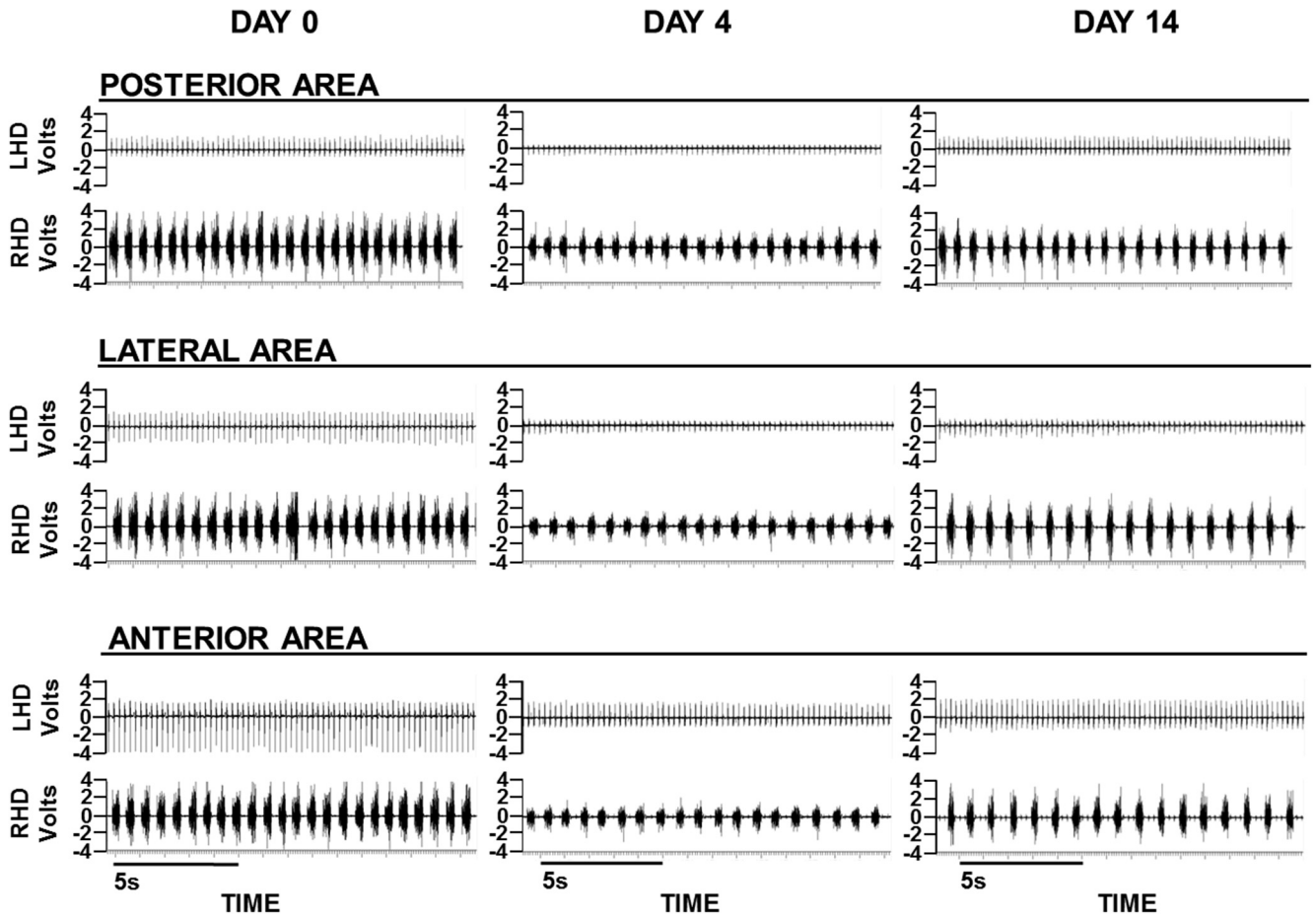

Figure 4. Representative EMG recordings of the posterior, lateral, and anterior areas of the LHD and RHD taken on day 0 (immediately following C2Hx) and 4 and 14 d after administration of the vehicle control containing WGA-HRP transporter conjugated to the gold nanoparticles (AuNP), WGA-HRP-AuNP. Amplitude of the EMG recordings, *y*-axis, is expressed in Volts. *x*-axis represents time, measured in seconds. Calibration: 5 s. Note that there is no activity in the LHD in any area and at any time.

jugate is transported exclusively to these nuclei in the spinal cord. There are no interneurons labeled in the cervical spinal cord. Figure 3*b* is a low-power image demonstrating bilateral WGA-HRP staining in the rVRG from the same animal. Figures 3*e* and 3*f* are higher-power images of these same cells of the left and right rVRG located in the medulla, respectively. The staining is localized to the neurons of the rVRG exclusively.

Characterization of the DPCPX nanoconjugate-induced diaphragmatic recovery

Figure 4 is a representative example of control EMG recordings from the left (ipsilateral to hemisection) and right (contralateral to hemisection) hemidiaphragms following the intradiaphagmatic administration of the vehicle control, WGA-HRP-AuNP (i.e., no drug) into the LHD. The vehicle was injected on day 0 (immediately after C2Hx) with recordings being shown from the same animal on day 0, day 4, and day 14 after the vehicle injection. Recordings are shown from the posterior, lateral, and anterior areas of the diaphragm. There is no activity in any area of the LHD at any time point, whereas the RHD is not affected by the hemisection. The single spikes observed in the LHD recordings are electrocardiogram activity, which progressively increases in amplitude as the sampling electrodes are moved toward more anterior areas of the LHD, close to the surface of the heart.

The effect of intradiaphragmatic administration of the nanoconjugate containing DPCPX on recovery of the diaphragm is presented in Figure 5. Immediately following confirmation of the hemidiaphragmatic paralysis, a one-time intradiaphragmatic injection of nanoconjugate containing 0.15 μg of the DPCPX drug per 1 kg of the animal's body weight induced recovery of the posterior, lateral, and anterior areas of the LHD. Typically, a complete paralysis of the LHD was observed on day 0, immediately after the C2Hx. Four days after administration of the DPCPX nanoconjugate, activity was detected in all three areas of the LHD. In other animals, the recovery was detected as early as 72 h after injection. In Fig. 5, the restored activity was synchronized with the activity in the RHD. Thus, the restored activity is respiratory-related. The recovery of the LHD persisted for 2 weeks after the one-time injection of the DPCPX nanoconjugate delivered on day 0. Similar recovery of the LHD was observed 4 weeks following the DPCPX nanoconjugate treatment, which was the longest period studied (data not shown; but see Fig. 9).

A dose-dependent recovery of the LHD function was noted after injection of 0.09, 0.15, and 0.27 μg/kg of DPCPX into separate groups of animals ($N = 10$ per group). Figure 6 shows representative EMG recordings obtained 14 d after treating the animals with these doses. In Figure 6, treatment with 0.09 μg/kg induced minimal, intermittent contractions observed in the lateral segment of the LHD on day 14. In the posterior segment of the diaphragm, an "augmented breath" (Bartlett, 1971) is visible within the 11th breath starting from the beginning of the recording. The augmented breath is visible within the intact RHD and

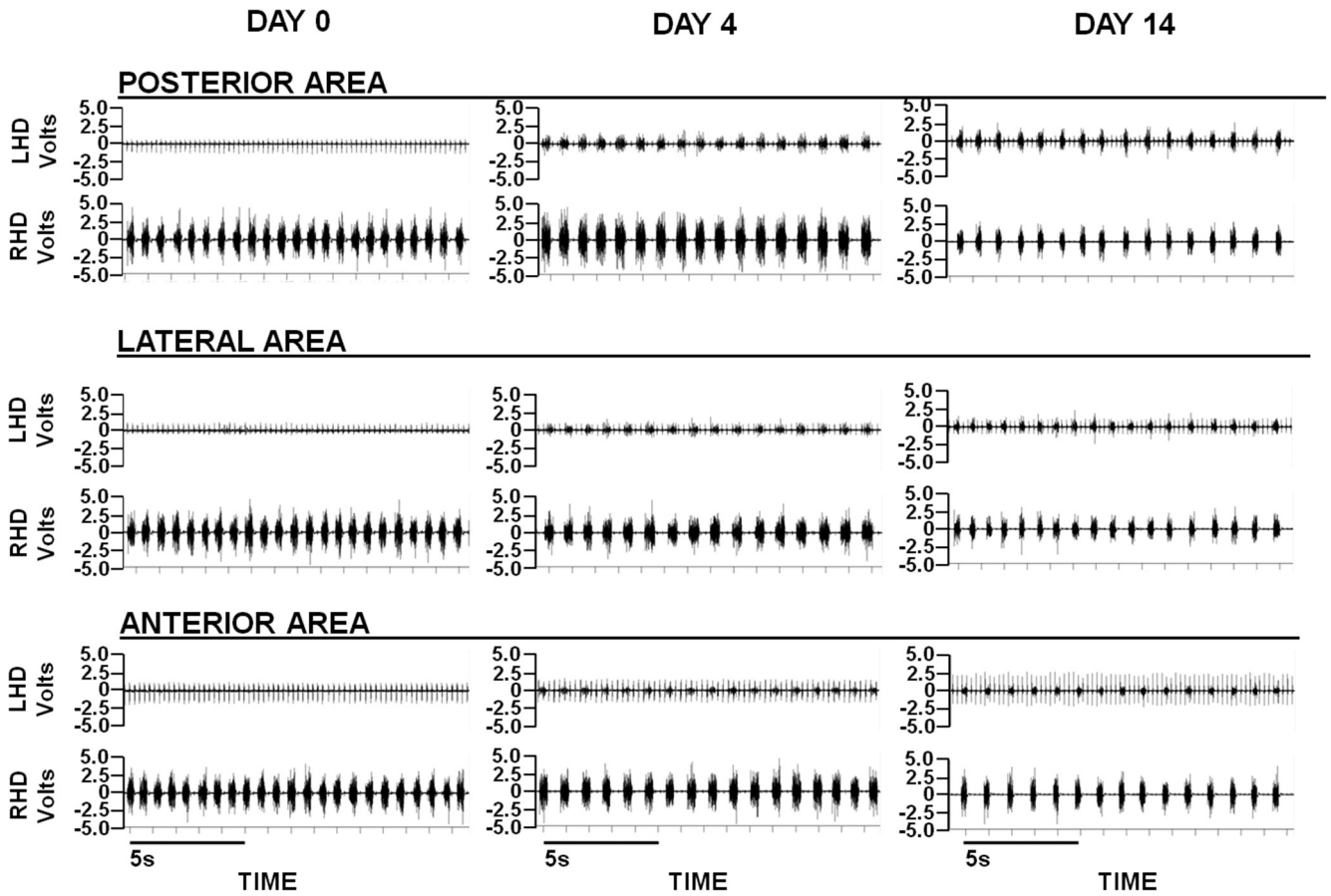

Figure 5. Representative EMG recordings of the posterior, lateral, and anterior areas of the LHD and RHD taken on day 0 and 4 and 14 d after intradiaphragmatic administration of 0.15 μg/kg of the DPCPX nanoconjugate. Amplitude of the EMG recordings, *y*-axis, is expressed in Volts. *x*-axis represents time, measured in seconds. Calibration: 5 s. Note recovery in all areas of the LHD starting on day 4 and persisting for 2 weeks.

also on the paralyzed LHD (arrows), suggesting that there are pathways other than the injured, descending bulbospinal pathways that are functional in the animal (e.g., the CPP). All animals, regardless of the treatment, displayed augmented breaths within the paralyzed LHD. This indicated that the latent crossed phrenic pathway was intact in all animals used and could be functionally expressed given the proper stimulus. From Figure 3, there were no interneurons labeled in the cervical spinal cord. Thus, the CPP (collaterals of the bulbospinal axons, which cross the midline of the spinal cord) is the most likely anatomical substrate for the recovery detected.

In this study, the incidence of "functional recovery" is defined as follows: (1) recovery that is detected in at least two of the three diaphragmatic areas; and (2) recovery that persists to the end of the study. Four of 10 (40%) rats that received a low dose of DPCPX nanoconjugate (0.09 μg/kg) displayed functional recovery of the paralyzed hemidiaphragm (Fig. 7). In animals treated with 0.15 μg/kg of DPCPX nanoconjugate, recovery was detected in 80% (8 of 10) of cases. In 6 of the 8 animals showing recovery, the activity of the entire diaphragm was restored, whereas in the remaining 2 animals recovery was confined to the posterior and lateral areas of the LHD. Finally, at the high dose of 0.27 μg/kg, the DPCPX nanoconjugate induced virtually no detectable recovery of the posterior segment of the LHD, but functional recovery, as defined above, was detected in 4 of 10 animals (Fig. 7).

Statistical significance of functional recovery detected with the EMG analysis was determined using the χ^2-Fisher's exact test followed by the Bonferroni adjustment. It should be stressed that here we are not assessing the amount of recovery, but rather the incidence of recovery in each treatment group with respect to the incidence of recovery in control animals (Fig. 7). The quantitative assessment of recovery was accomplished from phrenic nerve recordings in the section described below. Treatment with 0.15 μg/kg of DPCPX ($n = 10$) via intradiaphragmatic nanoconjugate delivery resulted in a significantly greater proportion of animals achieving functional recovery compared with vehicle controls ($n = 12$; $p = 0.001$). Therefore, this dose of the nanoconjugate was defined as "optimal." Treatment with 0.09 μg/kg ($n = 10$) or 0.27 μg/kg ($n = 10$) did not reach statistical significance ($p = 0.102$). The incidence of recovery in the optimal group was twice the incidence of recovery in both the low- and high-dose groups.

Quantitative assessments of DPCPX nanoconjugate-induced recovery of phrenic motor output

To quantify the amount of recovery induced by the DPCPX nanoconjugate, bilateral phrenic nerve recordings were performed 1 week ($n = 8$), 2 weeks 14 ($n = 8$), and 4 weeks ($n = 10$) in separate animals under physiologically standardized conditions according to procedures performed by many other laboratories (Baker-Herman and Mitchell, 2002; Nantwi and Goshgarian, 2002; Golder et al., 2003; Kajana and Goshgarian, 2008a; Lalley and Mifflin, 2012). The phrenic nerve recordings were taken after injection of the control nanoconjugate ($n = 13$)

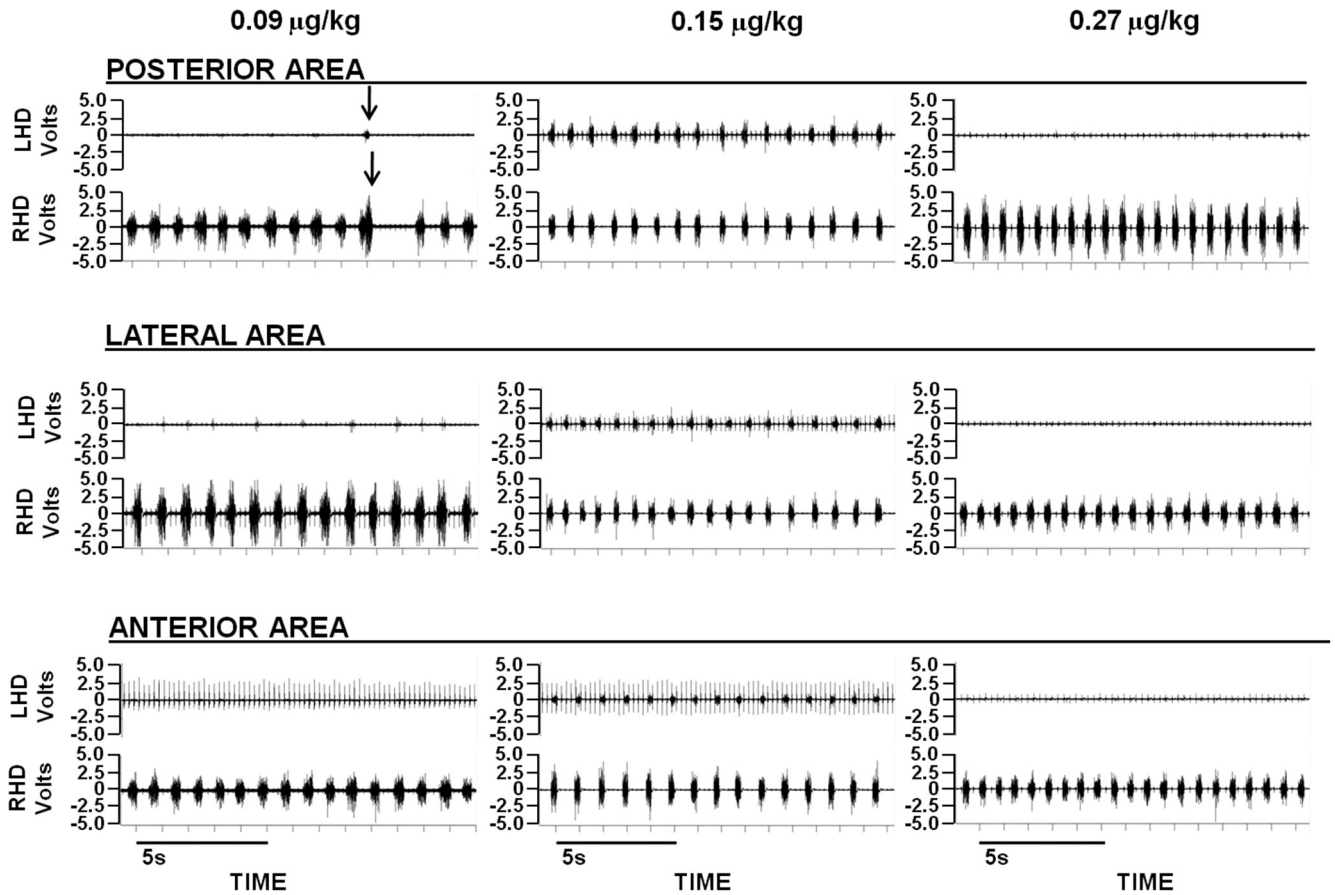

Figure 6. Representative examples of EMG recordings of the posterior, lateral, and anterior areas of the LHD and RHD measured on day 14 in three different animals receiving different doses of the DPCPX nanoconjugate. Animals received intradiaphragmatic injections of 0.09, 0.15, or 0.27 μg of the DPCPX nanoconjugate per kilogram of body weight on day 0. Top left panel, Arrow points to the augmented breath that appears in both the RHD and the paralyzed LHD, suggesting that there are latent pathways present. Amplitude of the EMG recordings, *y*-axis, is expressed in Volts. *x*-axis represents time, measured in seconds. Calibration: 5 s. Note marked recovery in the animal treated with 0.15 μg/kg of the DPCPX nanoconjugate in all three diaphragmatic areas, but very little recovery in the other animals.

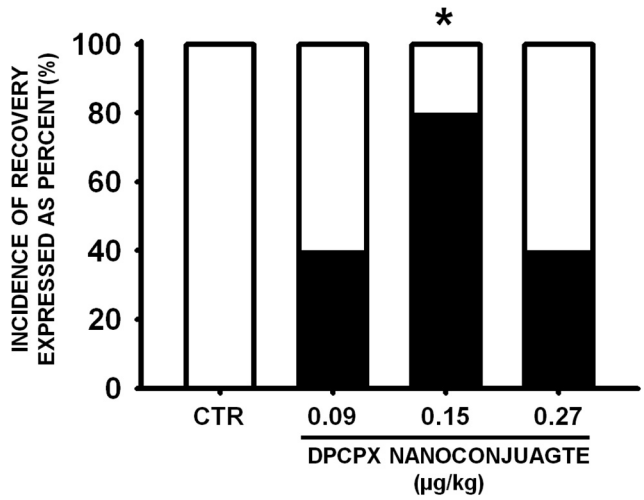

Figure 7. Vertical bar graphs represent the percentage of animals that did (black) and did not (white) exhibit recovery of LHD function upon treatment with vehicle control (CTR) or dose of 0.09, 0.15, or 0.27 μg/kg of the DPCPX nanoconjugate. The recovery was evaluated based on the criteria stated in Materials and Methods. The *p* value was adjusted for the number of comparisons based on the Bonferroni adjustment, where the α level of 0.016 was considered statistically significant. Note the statistically significant increase in percentage of animals (80%) that exhibited LHD recovery after injection of 0.15 μg/kg of DPCPX nanoconjugate. $^*p = 0.001$ versus CTR.

(WGA-HRP-AuNP) or in a separate group of animals after administration of the tripartite nanoconjugate ($n = 13$) (WGA-HRP-AuNP-DPCPX). The average blood pressure and temperature were maintained stable and within physiological ranges during the time of the recordings. Average blood pressure was 96.9 ± 6.1 mmHg, and the temperature was maintained at 37.1°C using a homeothermic blanket. Representative examples of phrenic nerve recordings 2 weeks after administration of control injections and 0.15 μg/kg of the DPCPX nanoconjugate (optimal dose) performed in separate animals are shown in Figure 8. Under control conditions, when the left C2Hx was followed by injection of a control nanoconjugate (i.e., WGA-HRP-AuNP), the RPN was functionally active, whereas the LPN was quiescent due to the hemisection (Fig. 8*A*). In the treatment group, delivery of the DPCPX nanoconjugate restored the activity of the LPN, and a representative example is shown in Figure 8*B*. The restored phasic activity of the LPN was synchronized with that of the RPN. Similarly, Figure 9 shows a representative phrenic nerve recording obtained 4 weeks after injection of (1) vehicle control, WGA-HRP-AuNP (Fig. 9*A*), and (2) optimal dose of DPCPX nanoconjugate (Fig. 9*B*). Importantly, 4 weeks following delivery of vehicle control, LPN is quiescent whereas RPN is functionally active. Acute administration of the optimal dose of the DPCPX nanoconjugate resulted in recovery of LPN activity as long as 4 weeks after C2Hx. Importantly LPN activity was quiescent after administration of the vehicle control at all time points tested (1, 2,

and 4 weeks after C2Hx), whereas LPN activity was restored at all time points in animals treated with the DPCPX nanoconjugate.

To quantitate the phrenic motor output, the areas under the curves (AUC) of 10 consecutive rectified and integrated waveforms of the LPN and RPN bursts as well as their maximal amplitudes were averaged. The activity in the LPN was expressed as the percentage of the RPN whose signal was set to be 100%. Statistical analyses were performed using two-way ANOVA to analyze the effect of drug (factor 1) and time (factor 2) on recovery of LPN activity. Treatment resulted in a significant recovery of LPN activity for both the AUC ($p = 0.001$) and the maximum amplitude ($p = 0.001$); however, time had no effect on the AUC or maximum amplitude observed ($p = 0.068$). Student's *t* test revealed a statistically significant difference between the AUC of DPCPX-treated and control animals at 1, 2, and 4 weeks ($p = 0.009$). At week 1, the mean AUC for DPCPX-treated animals was 56.8 ± 4.3%, whereas the mean for controls was 8.2 ± 2.3%. At weeks 2 and 4, the mean AUCs for the treated groups were 72.4 ± 7.3% and 46.5 ± 11.8%, respectively, which was not significantly different from the mean AUC observed at earlier time points (Fig. 10). Student's *t* test also revealed a significant difference in the maximum amplitude between DPCPX-treated and control groups at 1, 2, and 4 weeks following the injury ($p = 0.009$). At 1 week, maximum amplitude of DPCPX-treated animals was 75.7 ± 6.6%, whereas the maximum amplitude for the control was 9.3 ± 2.8%. The maximum amplitude of DPCPX-treated animals remained about the same at 2 and 4 weeks and was statistically greater than controls (Fig. 10).

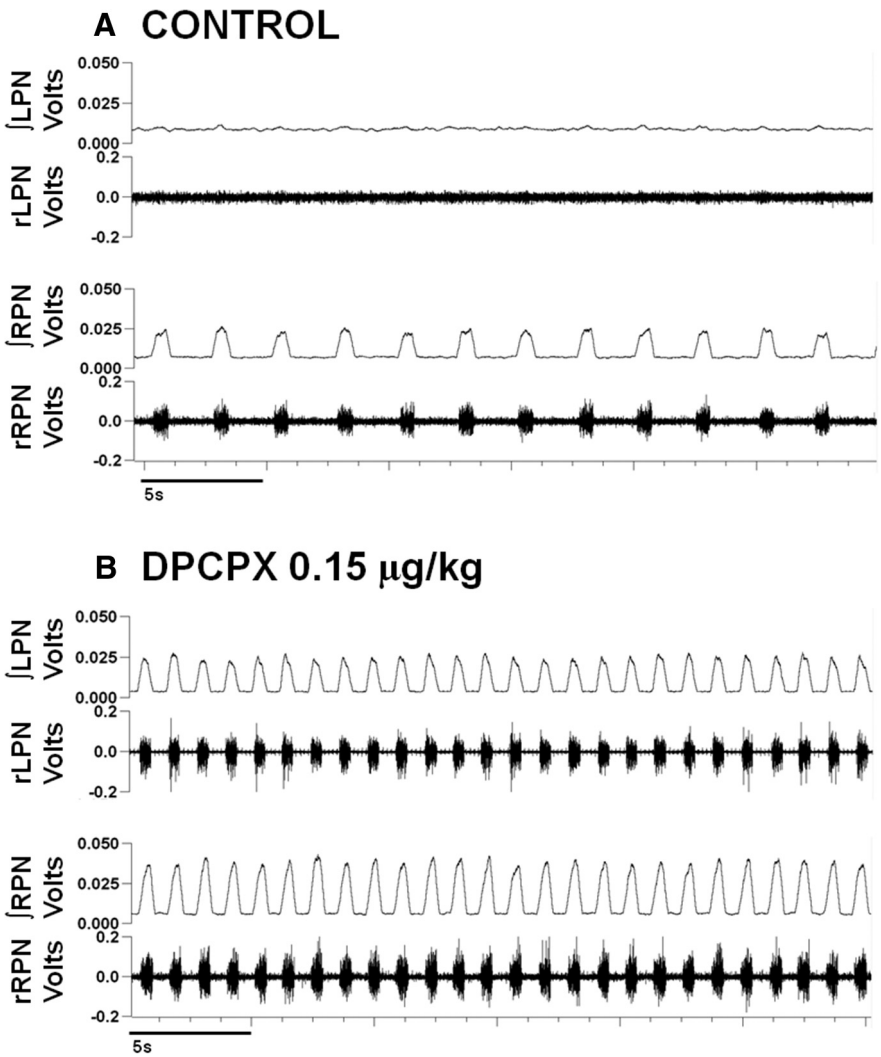

Figure 8. Representative examples of the bilateral raw (r) and integrated (∫) phrenic nerve recording obtained under standardized physiological conditions on day 14 in (***A***) control setting, after administration of vehicle control, WGA-HRP-AuNP; and (***B***) after delivery of the 0.15 μg/kg of the DPCPX nanoconjugate. Amplitude of the phrenic nerve recordings (*y*-axis) is expressed in Volts. *x*-axis represents time, measured in seconds. ∫LPN, Integrated left phrenic nerve; rLPN, raw left phrenic nerve; ∫RPN, integrated right phrenic nerve; rRPN, raw right phrenic nerve. Note recovery of the LPN in the DPCPX-treated rat.

Effect of DPCPX nanoconjugate on respiratory frequency

During phrenic nerve recording, under standardized conditions, frequency was analyzed in control animals ($n = 13$) and in DPCPX-treated animals ($n = 13$) 1, 2, and 4 weeks following injection of the optimal dose of the DPCPX nanoconjugate (0.15 μg/kg) or following injection of vehicle control (WGA-HRP-AuNP). The analysis revealed a significant effect of treatment (factor 1) on the respiratory frequency ($p = 0.001$). ANOVA also revealed no statistical difference for the effect of time (factor 2) on this parameter ($p = 0.2$). Furthermore, specific pairwise analysis using Student's *t* test showed that, 1 and 2 weeks following the DPCPX treatment, the animals exhibited a statistically significant increase in respiratory frequency ($p = 0.001$) compared with the control animals. The frequency at week 1 was 39 ± 1 breaths per minute (bpm) and at week 2, 43 ± 1 bpm compared with the control animals, which inspired 28 ± 3 times in 1 min. Week 4 analyses showed no difference in frequency between the control and DPCPX-treated animals, and this was largely due to increase in respiratory frequency in control animals (35 ± 3 bpm vs 28 ± 3 at week 1). Mean respiratory frequency in uninjured animals treated with DPCPX nanoconjugate was 39 ± 1 bpm (Table 1).

Discussion

The major finding of this study is that the selective delivery of an A1 adenosine receptor antagonist to central respiratory pathways induced recovery of respiratory-related function lost after SCI. A one-time series of intradiaphragmatic injections of the DPCPX nanoconjugate induced long-lasting recovery of the paralyzed LHD. Functional recovery was achieved using only a small fraction of the effective dose of DPCPX required when given systemically in previous studies (Nantwi et al., 2003). A dose–response study revealed that the optimal dose of DPCPX delivered via nanoconjugate was 0.15 μg/kg, which is only 0.1% of the systemic therapeutic dose. In a placebo-controlled, double-blind crossover study investigating the effects of theophylline on recovery of respiratory motor function in patients after SCI, failure to detect improvements was attributed to the small number of participants

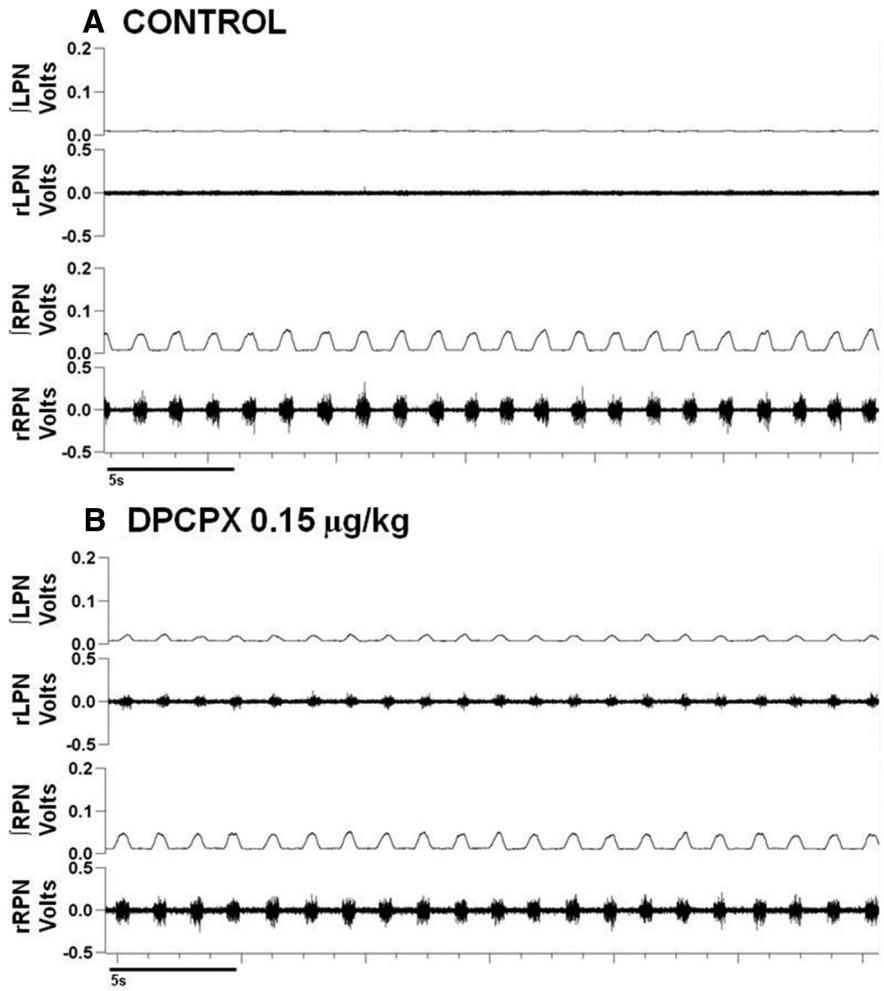

Figure 9. Representative examples of the bilateral raw (r) and integrated (∫) phrenic nerve recording obtained under standardized physiological conditions 4 weeks following injection of (***A***) vehicle control and (***B***) after delivery of the 0.15 μg/kg of DPCPX nanoconjugate. Amplitude of the phrenic nerve recordings (*y*-axis) is expressed in Volts. *x*-axis represents time, measured in seconds. ∫LPN, Integrated left phrenic nerve; rLPN, raw left phrenic nerve; ∫RPN, integrated right phrenic nerve; rRPN, raw right phrenic nerve. Note recovery of the LPN in the DPCPX-treated rat.

able to tolerate the systemic side effects caused by the drug (Tzelepis et al., 2006). Therefore, the ability of the present drug delivery approach to reduce the effective drug dose represents a major advancement in the field, and it provides renewed potential to treat respiratory dysfunction after SCI with drugs previously not well tolerated.

We have demonstrated that selective antagonism of A1 adenosine receptors improves respiratory-related activity following C2Hx and have shown that antagonism of the A_2 adenosine receptor subtype is not involved in this phenomenon (Nantwi and Goshgarian, 2002). The recovery observed in the present study is physiologically very similar to the recovery observed following systemic administration of DPCPX leading to activation of the cAMP-PKA pathway (Kajana and Goshgarian, 2008b). Furthermore, DPCPX has been used by numerous laboratories to inhibit A1 adenosine receptors, and pharmacodynamic studies suggest that DPCPX is 700-fold more selective for binding A1 receptor compared with the other adenosine receptor subtypes (Lee and Reddington, 1986; Coates et al., 1994). Taking all the evidence together and comparing the similarities between the results obtained in the studies in which DPCPX was administered systemically and the present study where the antagonist was delivered using nanotechnology approach, we conclude that the observed effects are due to the specific antagonism of A1 adenosine receptors.

It was originally thought that adenosine receptor antagonists, including DPCPX, bind to the extracellular loop of the A1 adenosine receptor. However, other findings have shown that the ligand binding site may be away from the outer membrane surface (Ijzerman et al., 1992; Olah et al., 1994; Rivkees et al., 1999). Accordingly, our current hypothesis is that intracellularly delivered DPCPX can act on the intracellular regions of the protein. Another possibility is that the antagonist may act on newly synthesized A1 adenosine receptors not yet trafficked to the membrane surface. In accordance with this hypothesis, Schmidt et al. (1995) observed alterations in respiratory output following intracellular injection of adenosine into rVRG neurons. Therefore, it seems plausible that adenosine receptor inhibitors similarly elicit antagonistic effects when administered intracellulary.

Dose–response studies using the DPCPX nanoconjugate revealed a bell-shaped curve where both lower and higher doses of the nanconjugate had minimal effect on diaphragmatic activity, whereas a dose of 0.15 μg/kg yielded optimal recovery. The bell shape response may be due to the specific nature of this adenosine receptor antagonist. We have reported similar observations in our previous studies where higher doses of theophylline suppressed respiratory drive to the injured hemidiaphragm (Nantwi et al., 1996). This biphasic effect is likely due to differential actions of specific adenosine receptor antagonist on different receptor subtypes, which exert opposing effects on neurotransmitter release. This observation is very important as it relates to the therapeutic window of xanthine derivatives when delivered using this nanotechnology approach and could have future clinical implications.

Previous studies from our laboratory observed spontaneous respiratory-related activity in the C2Hx rat model at ~6 weeks after injury (Nantwi et al., 1999). However, others have reported spontaneous recovery as early as 14 d after the injury in the same animal model (Fuller et al., 2008; Gransee et al., 2015). We performed a control set of experiments and observed minimal spontaneous recovery occurring during the first 4 weeks following C2Hx. Therefore, we performed our physiological studies to 4 weeks and found that a single administration of DPCPX nanoconjugate will induce long-lasting recovery for 4 weeks following the injury. Quantitative analyses suggest that the amount of recovery was similar to the amount observed 1 week following the drug administration. Additionally, ~4 weeks after SCI, many animals exhibit autophagy of the contralateral hindpaw, thereby making further extension of the studies inhumane. Within that scope, administration of the DPCPX nanoconjugate induced early, long-lasting recovery of diaphragm function paralyzed after SCI.

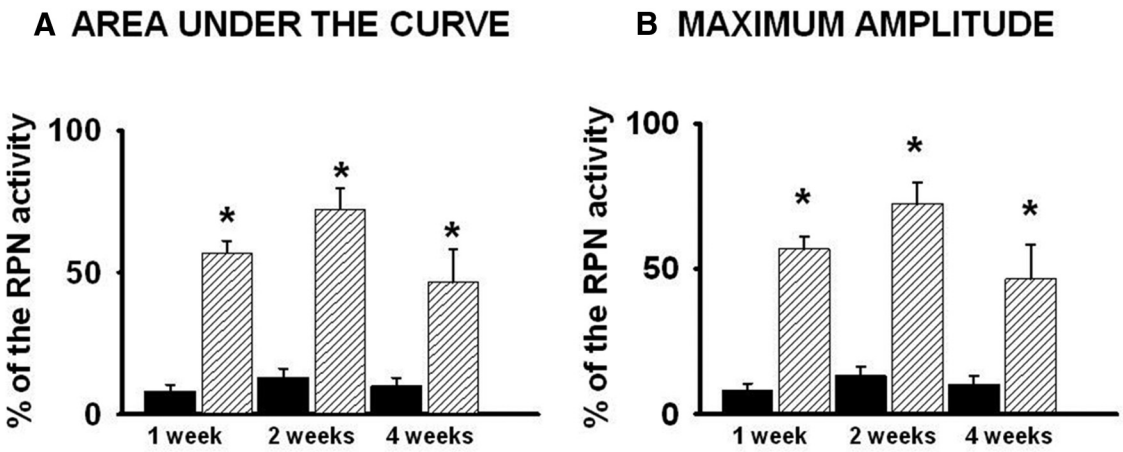

Figure 10. Averaged phrenic nerve recording data, which are expressed as mean ± SE. Solid black bars represent data obtained under control conditions, after administration of the WGA-HRP-AuNP control. Dashed bars represent the values obtained after treatment with the 0.15 μg/kg DPCPX nanoconjugate. ***A***, Mean data for the area under the curve. ***B***, Mean data for the change in amplitudes quantified 1, 2, and 4 weeks after intradiaphragmatic injections. Areas under the 10 consecutive LPN and RPN curves as well as the maximal amplitude under these same breaths were analyzed and averaged. The activity in the LPN is expressed as percentage of the activity in the RPN. *$p < 0.001$ versus control.

Table 1. Effect of DPCPX nanoconjugate administration on the respiratory frequency in naive, and C2Hx animals 1, 2, and 4 weeks following the injury[a]

Naive animals	Control[b] 1 week	DPCPX 1 week	Control[b] 2 weeks	DPCPX 2 weeks	Control[b] 4 weeks	DPCPX 4 weeks
39 ± 1	28 ± 1	39 ± 3*	28 ± 3	43 ± 1*	35 ± 3	40 ± 2

[a]Values are breaths per minute.

[b]Control animals received WGA-HRP-AuNP construct (no drug).

*$p < 0.01$ versus control.

There have been other studies investigating the effects of intermittent hypoxia therapy both in animal models and in humans to improve respiratory function after SCI (Baker and Mitchell, 2000; Fuller et al., 2000; Golder and Mitchell, 2005; Wilkerson and Mitchell, 2009; Tester et al., 2014). While acute intermittent hypoxia is a minimally invasive approach that facilitates phrenic motor output, the effect of a single cycle of acute intermittent hypoxia is short-term. Similarly, optogenetic approaches have been used in which intermittent phototherapy induces recovery of diaphragm function after SCI (Alilain et al., 2008). This approach restores diaphragmatic activity that persists for several minutes after which the ipsilateral hemidiaphragm becomes paralyzed once again due to the hemisection. Indeed, there are no available reports on duration of recovery lasting longer than several days, other than from our own laboratory (Nantwi and Goshgarian, 2002; present paper). Furthermore, cell-based approaches targeting brain-derived neurotrophic factor and tropomyosin related kinase receptor 2subtype B or choindritinase ABC inhibition were able to demonstrate recovery of respiratory function after SCI (Mantilla et al., 2013; Gransee et al., 2015); however, further studies are needed to address the potential for translation of such methods to clinical use. Finally, some reports suggest that diaphragm pacing and abdominal binder placement improved respiratory-related function after SCI (Tedde et al., 2012; Wadsworth et al., 2012; Posluszny et al., 2014). To our knowledge, however, the present study is the first to demonstrate the ability of a nanotechnology approach to induce long-lasting recovery of respiratory function after spinal cord injury.

Because WGA-HRP, which transports AuNP-DPCPX, was visualized within the neurons of the rVRG and the phrenic nucleus, we rationalized that DPCPX-induced recovery is mostly mediated via activation of the neurons within these respiratory centers. However, it is plausible for the nanoconjugate to be transsynaptically carried across more than one synapse and modulate activity within the respiratory centers higher than the rVRG. However, we have previously shown that intradiaphragmatic administration of a similar transporter, WGA-Alexa-488, results in labeling of rVRG neurons without labeling other supraspinal centers when the transporter was administered acutely following C2Hx (Buttry and Goshgarian, 2014). In the chronic hemisection model, however, intradiaphragm administration of the transporter resulted in labeling of rVRG in addition to the raphe, hypoglossal, spinal trigeminal, parvicellular reticular, gigantocellular reticular, and intermediate reticular nuclei (Buttry and Goshgarian, 2014).

Based on the fact that retrograde transsynaptic transport of WGA-HRP was confirmed 48 h following the transporter administration (Jankowska, 1985; Harrison et al., 1986; Moreno et al., 1992), we suggest that the recovery occurring as early as 72 h after the nanoconjugate injection is a result of the time required for the adequate transport of the nanoconjugate to the respiratory centers plus the time required for release of the drug into targeted neurons. In support of this hypothesis, the nanoconjugate is designed such that the drug portion is linked to the remaining construct by an ester bond, which allows for hydrolytic degradation of the drug from the construct following the injection. We hypothesize that, once the drug is released, its pharmacokinetic profile remains unaltered. That is, the half-time of DPCPX is 2.36 h (Lu et al., 2014). Therefore, we expect the drug to be metabolized and cleared from the system within hours upon release. However, during this time, DPCPX makes permanent changes to the respiratory circuitry, which results in long-term respiratory recovery in the virtual absence of the drug from the animal. A similar result was observed following the chronic administration of theophylline. When the animal was weaned from theophylline, the respiratory recovery persisted (Nantwi et al., 2003). Additionally, we are currently undertaking a biodistribution study to understand trafficking of the gold nanoparticles following disassociation of the drug from the construct.

Given that the transport of WGA-HRP is dependent upon the presence of physiologically active synapses, which act as a substrate to drive delivery of the drug to the respiratory centers, and taking into account previous studies implicating the synapses of the CPP pathway in adenosine-mediated respiratory recovery, we rationalized that the DPCPX nanoconjugate-induced recovery also activates the latent CPP pathway. However, there are other possible explana-

tions, including the involvement of cervical interneurons, which may contribute to DPCPX nanoconjugate-induced recovery of respiratory function following C2Hx (Lane et al., 2008, 2009). In our previous study where WGA-HRP was injected into the paralyzed, LHD during activation of the crossed phrenic pathway, no interneurons were labeled in the cervical spinal cord, making this possibility unlikely (Moreno et al., 1992).

In the current study, both the amplitude and the AUC of the LPN (ipsilateral to hemisection) were increased by treatment with the DPCPX nanoconjugate, suggesting potential for the drug to induce global respiratory motor recovery of the cells within the respiratory network. Specifically, we demonstrated that by 1 week, the DPCPX nanoconjugate treatment restored 57% of the respiratory drive to the LPN; and on week 2, this recovery was ~72%. Two weeks later, the amount of restored respiratory drive was 47%. These values are similar to what was reported in our previous studies using systemic administration of DPCPX (Nantwi and Goshgarian, 2002). These findings may be explained by the dense expression of adenosine A1 receptors on the neurons within the central respiratory centers, phrenic nucleus, and in the rVRG (Petrov et al., 2007). Therefore, because of the action of the drug on the widely distributed A1 adenosine receptors, we were able to achieve a marked increase in the LPN output after SCI in the present study. Finally, the global expression of the A1 receptors within the respiratory networks also governs minute effective concentrations of the drug used via selective targeting approached developed in the study. In addition to having effects on the respiratory output, DPCPX nanoconjugate increased respiratory frequency. The respiratory frequency was increased at 1 and 2 weeks following the administration of the nanoconjugate in C2Hx and naive animals. These data are consistent with previously established respiratory effects induced by A1 adenosine antagonists and further support the conclusion that the recovery is indeed mediated via this receptor subtype (Nantwi and Goshgarian, 2002). Additionally, the increases in respiratory frequency may be consequence of the drug action on the cells within the Botzinger complex. There are two possibilities, which may explain how effects of the nanoconjugate delivery to the rVRG could impact neurons of the Botzinger complex: (1) activation of neurons within the rVRG projecting to the Botzinger complex; or (2) the drug may diffuse to the pre-Botzinger complex and directly activate neurons there. Indeed, analyses of the respiratory frequency suggest that delivery of the DPCPX nanoconjugate increases respiratory frequency, which may be due to actions of the drug on the neurons within the Botzinger complex (Weston et al., 2004; Tan et al., 2010) Importantly, there is a considerable anatomical and functional overlap between the neurons of the rVRG and pre-Botzinger complex, which makes decoding of specific effect on either one of the nuclei difficult (Sun et al., 1998).

In conclusion, in the present study, we have demonstrated that a single delivery of adenosine A1 receptor antagonist via a nanotechnology approach induces virtually permanent recovery, which persists up to 4 weeks following the single drug administration. Given the ability of the CPP to supply central drive to the paralyzed hemidiaphragm via decussation at the level of the phrenic nucleus, it is reasonable to expect continued recovery of respiratory drive to the LHD through the use of this therapeutic approach. We think that this method of delivering the drugs would be a clinically feasible approach that patients would consent to given the high importance of alleviating respiratory dysfunction to this patient population.

References

Alilain WJ, Li X, Horn KP, Dhingra R, Dick TE, Herlitze S, Silver J (2008) Light-induced rescue of breathing after spinal cord injury. J Neurosci 28:11862–11870. CrossRef Medline

Aserinsky E (1961) Effects of usage of a dormant respiratory nerve pathway upon its subsequent activity. Exp Neurol 3:467–475. CrossRef Medline

Baker TL, Mitchell GS (2000) Episodic but not continuous hypoxia elicits long-term facilitation of phrenic motor output in rats. J Physiol 529: 215–219. CrossRef Medline

Baker-Herman TL, Mitchell GS (2002) Phrenic long-term facilitation requires spinal serotonin receptor activation and protein synthesis. J Neurosci 22:6239–6246. Medline

Barnes PJ (2013) Theophylline. Am J Respir Crit Care Med 188:901–906. CrossRef Medline

Bartlett D Jr (1971) Origin and regulation of spontaneous deep breaths. Respir Physiol 12:230–238. CrossRef Medline

Bascom AT, Lattin CD, Aboussouan LS, Goshgarian HG (2005) Effect of acute aminophylline administration on diaphragm function in high cervical tetraplegia: a case report. Chest J 127:658–661. CrossRef Medline

Buttry JL, Goshgarian HG (2014) Injection of WGA-Alexa 488 into the ipsilateral hemidiaphragm of acutely and chronically C2 hemisected rats reveals activity-dependent synaptic plasticity in the respiratory motor pathways. Exp Neurol 261:440–450. CrossRef Medline

Coates J, Sheehan MJ, Strong P (1994) 1,3-Dipropyl-8-cyclopentyl xanthine (DPCPX): a useful tool for pharmacologists and physiologists? Gen Pharmacol 25:387–394. CrossRef Medline

DeVries KL, Goshgarian HG (1989) Spinal cord localization and characterization of the neurons which give rise to the accessory phrenic nerve in the adult rat. Exp Neurol 104:88–90. CrossRef Medline

Dreaden EC, Mackey MA, Huang X, Kang B, El-Sayed MA (2011) Beating cancer in multiple ways using nanogold. Chem Soc Rev 40:3391–3404. CrossRef Medline

Etheridge ML, Campbell SA, Erdman AG, Haynes CL, Wolf SM, McCullough J (2013) The big picture on nanomedicine: the state of investigational and approved nanomedicine products. Nanomed Nanotechnol 9:1–14. CrossRef Medline

Ferguson GT, Khanchandani N, Lattin CD, Goshgarian HG (1999) Clinical effects of theophylline on inspiratory muscle drive in tetraplegia. Neurorehabil Neural Repair 13:191–197. CrossRef

Fuller DD, Bach KB, Baker TL, Kinkead R, Mitchell GS (2000) Long term facilitation of phrenic motor output. Respir Physiol 121:135–146. CrossRef Medline

Fuller DD, Doperalski NJ, Dougherty BJ, Sandhu MS, Bolser DC, Reier PJ (2008) Modest spontaneous recovery of ventilation following chronic high cervical hemisection in rats. Exp Neurol 211:97–106. CrossRef Medline

Golder FJ, Mitchell GS (2005) Spinal synaptic enhancement with acute intermittent hypoxia improves respiratory function after chronic cervical spinal cord injury. J Neurosci 25:2925–2932. CrossRef Medline

Golder FJ, Fuller DD, Davenport PW, Johnson RD, Reier PJ, Bolser DC (2003) Respiratory motor recovery after unilateral spinal cord injury: eliminating crossed phrenic activity decreases tidal volume and increases contralateral respiratory motor output. J Neurosci 23:2494–2501. Medline

Gransee HM, Zhan WZ, Sieck GC, Mantilla CB (2015) Localized delivery of brain-derived neurotrophic factor-expressing mesenchymal stem cells enhances functional recovery following cervical spinal cord injury. J Neurotrauma 32:185–193. CrossRef Medline

Guth L (1976) Functional plasticity in the respiratory pathway of the mammalian spinal cord. Exp Neurol 51:414–420. CrossRef Medline

Harrison PJ, Jankowska E, Zytnicki D (1986) Lamina VIII interneurones interposed in crossed reflex pathways in the cat. J Physiol 371:147–166. CrossRef Medline

Ijzerman AP, van Galen PJ, Jacobson KA (1992) Molecular modeling of adenosine receptors: I. The ligand binding site on the A1 receptor. Drug Des Disc 9:49. Medline

Jana NR, Gearheart L, Murphy CJ (2001) Wet chemical synthesis of high aspect ratio cylindrical gold nanorods. J Phys Chem B 105:4065–4067. CrossRef

Jankowska E (1985) Further indications for enhancement of retrograde transneuronal transport of WGA-HRP by synaptic activity. Brain Res 341:403–408. CrossRef Medline

Kajana S, Goshgarian HG (2008a) Administration of phosphodiesterase inhibitors and an adenosine A1 receptor antagonist induces phrenic nerve recovery in high cervical spinal cord injured rats. Exp Neurol 210:671–680. CrossRef Medline

Kajana S, Goshgarian HG (2008b) Spinal activation of the cAMP-PKA pathway induces respiratory motor recovery following high cervical spinal cord injury. Brain Res 1232:206–213. CrossRef Medline

Kajana S, Goshgarian HG (2009) Systemic administration of rolipram in-

creases medullary and spinal cAMP and activates a latent respiratory motor pathway after high cervical spinal cord injury. J Spinal Cord Med 32:175–182. Medline

Lalley PM, Mifflin SW (2012) Opposing effects on the phrenic motor pathway attributed to dopamine-D1 and-D3/D2 receptor activation. Respir Physiol Neurobiol 181:183–193. CrossRef Medline

Lane MA, White TE, Coutts MA, Jones AL, Sandhu MS, Bloom DC, Bolser DC, Yates BJ, Fuller DD, Reier PJ (2008) Cervical prephrenic interneurons in the normal and lesioned spinal cord of the adult rat. J Comp Neurol 511:692–709. CrossRef Medline

Lane MA, Lee KZ, Fuller DD, Reier PJ (2009) Spinal circuitry and respiratory recovery following spinal cord injury. Respir Physiol Neurobiol 169: 123–132. CrossRef Medline

Lee KS, Reddington M (1986) 1,3-Dipropyl-8-cyclopentylxanthine (DPCPX) inhibition of [3 H] N-ethylcarboxamidoadenosine (NECA) binding allows the visualization of putative non-A1 adenosine receptors. Brain Res 368:394–398. CrossRef Medline

Lohse MJ, Klotz KN, Lindenborn-Fotinos J, Reddington M, Schwabe U, Olsson RA (1987) 8-Cyclopentyl-1,3-dipropylxanthine (DPCPX): a selective high affinity antagonist radioligand for A1 adenosine receptors. Naunyn Schmiedebergs Arch Pharmacol 336:204–210. CrossRef Medline

Lu M, Wang B, Zhang C, Zhuang X, Yuan M, Wang H, Li W, Su R, Li J (2014) PQ-69, a novel and selective adenosine A1 receptor antagonist with inverse agonist activity. Purinergic Signal 10:619–629. CrossRef Medline

Mantilla CB, Gransee HM, Zhan WZ, Sieck GC (2013) Motoneuron BDNF/TrkB signaling enhances functional recovery after cervical spinal cord injury. Exp Neurol 247:101–109. CrossRef Medline

Mieszawska AJ, Mulder WJ, Fayad ZA, Cormode DP (2013) Multifunctional gold nanoparticles for diagnosis and therapy of disease. Mol Pharm 10:831–847. CrossRef Medline

Moreno DE, Yu XJ, Goshgarian HG (1992) Identification of the axon pathways which mediate functional recovery of a paralyzed hemidiaphragm following spinal cord hemisection in the adult rat. Exp Neurol 116: 219–228. CrossRef Medline

Nantwi KD, Goshgarian HG (2002) Actions of specific adenosine receptor A1 and A2 agonists and antagonists in recovery of phrenic motor output following upper cervical spinal cord injury in adult rats. Clin Exp Pharmacol Physiol 29:915–923. CrossRef Medline

Nantwi KD, Goshgarian HG (2005) Adenosinergic mechanisms underlying recovery of diaphragm motor function following upper cervical spinal cord injury: potential therapeutic implications. Neurol Res 27:195–205. CrossRef Medline

Nantwi KD, El-Bohy AA, Schrimsher GW, Reier PJ, Goshgarian HG (1999) Spontaneous functional recovery in a paralyzed hemidiaphragm following upper cervical spinal cord injury in adult rats. Neurorehabil Neural Repair 13:225–234. CrossRef

Nantwi KD, Basura GJ, Goshgarian HG (2003) Effects of long-term theophylline exposure on recovery of respiratory function and expression of adenosine A1 mRNA in cervical spinal cord hemisected adult rats. Exp Neurol 182:232–239. CrossRef Medline

Nantwi KD, El-Bohy A, Goshgarian HG (1996) Actions of systemic theophylline on hemidiaphragmatic recovery in rats following cervical spinal cord hemisection. Exp Neurol 140:53–59. CrossRef Medline

Olah ME, Jacobson KA, Stiles GL (1994) Role of the second extracellular loop of adenosine receptors in agonist and antagonist binding: analysis of chimeric A1/A3 adenosine receptors. J Biol Chem 269:24692–24698. Medline

Petrov T, Kreipke C, Alilain W, Nantwi KD (2007) Differential expression of adenosine A1 and A2A receptors after upper cervical (C2) spinal cord hemisection in adult rats. J Spinal Cord Med 30:331–337. Medline

Posluszny JA Jr, Onders R, Kerwin AJ, Weinstein MS, Stein DM, Knight J, Lottenberg L, Cheatham ML, Khansarinia S, Dayal S, Byers PM, Diebel L (2014) Multicenter review of diaphragm pacing in spinal cord injury: successful not only in weaning from ventilators but also in bridging to independent respiration. J Trauma Acute Care Surg 76:303–310. CrossRef Medline

Rivkees SA, Barbhaiya H, IJzerman AP (1999) Identification of the adenine binding site of the human A1 adenosine receptor. J Biol Chem 274:3617–3621. CrossRef Medline

Schmidt C, Bellingham MC, Richter DW (1995) Adenosinergic modulation of respiratory neurones and hypoxic responses in the anaesthetized cat. J Physiol 483:769–781. CrossRef Medline

Sloan KB, Bodor N (1982) Hydroxymethyl and acyloxymethyl prodrugs of theophylline: enhanced delivery of polar drugs through skin. Int J Pharm 12:299–313. CrossRef

Strack AM, Loewy AD (1990) Pseudorabies virus: a highly specific transneuronal cell body marker in the sympathetic nervous system. J Neurosci 10:2139–2147. Medline

Sun QJ, Goodchild AK, Chalmers JP, Pilowsky PM (1998) The pre-Bötzinger complex and phase-spanning neurons in the adult rat. Brain Res 809:204–213. CrossRef Medline

Tan W, Pagliardini S, Yang P, Janczewski WA, Feldman JL (2010) Projections of pre-Bötzinger complex neurons in adult rats. J Comp Neurol 518:1862–1878. CrossRef Medline

Tedde ML, Vasconcelos Filho P, Hajjar LA, de Almeida JP, Flora GF, Okumura EM, Osawa EA, Fukushima JT, Teixeira MJ, Galas FR, Jatene FB, Auler JO Jr (2012) Diaphragmatic pacing stimulation in spinal cord injury: anesthetic and perioperative management. Clinics 67:1265–1269. CrossRef Medline

Tester NJ, Fuller DD, Fromm JS, Spiess MR, Behrman AL, Mateika JH (2014) Long-term facilitation of ventilation in humans with chronic spinal cord injury. Am J Respir Crit Care Med 189:57–65. CrossRef Medline

Tzelepis GE, Bascom AT, Safwan Badr M, Goshgarian HG (2006) Effects of theophylline on pulmonary function in patients with traumatic tetraplegia. J Spinal Cord Med 29:227–233. Medline

Wadsworth BM, Haines TP, Cornwell PL, Rodwell LT, Paratz JD (2012) Abdominal binder improves lung volumes and voice in people with tetraplegic spinal cord injury. Arch Phys Med Rehabil 93:2189–2197. CrossRef Medline

Weston MC, Stornetta RL, Guyenet PG (2004) Glutamatergic neuronal projections from the marginal layer of the rostral ventral medulla to the respiratory centers in rats. J Comp Neurol 473:73–85. CrossRef Medline

Wilkerson JE, Mitchell GS (2009) Daily intermittent hypoxia augments spinal BDNF levels, ERK phosphorylation and respiratory long-term facilitation. Exp Neurol 217:116–123. CrossRef Medline

Winslow C, Rozovsky J (2003) Effect of spinal cord injury on the respiratory system. Am J Phys Med Rehabil 82:803–814. CrossRef Medline